

Sulfide Oxidation across Diffuse Flow Zones of Hydrothermal Vents

Amy Gartman · Mustafa Yücel · Andrew S. Madison · David W. Chu · Shufen Ma · Christopher P. Janzen · Erin L. Becker · Roxanne A. Beinart · Peter R. Girguis · George W. Luther III

Received: 11 January 2011 / Accepted: 30 April 2011 / Published online: 31 May 2011
© Springer Science+Business Media B.V. 2011

Abstract The sulfide ($\text{H}_2\text{S}/\text{HS}^-$) that is emitted from hydrothermal vents begins to oxidize abiotically with oxygen upon contact with ambient bottom water, but the reaction kinetics are slow. Here, using in situ voltammetry, we report detection of the intermediate sulfur oxidation products polysulfides [S_x^{2-}] and thiosulfate [$\text{S}_2\text{O}_3^{2-}$], along with contextual data on sulfide, oxygen, and temperature. At Lau Basin in 2006, thiosulfate was identified in less than one percent of approximately 10,500 scans and no polysulfides were detected. Only five percent of 11,000 voltammetric scans taken at four vent sites at Lau Basin in

A. Gartman (✉) · M. Yücel · A. S. Madison · S. Ma · G. W. Luther III
School of Marine Science and Policy, College of Earth, Ocean and Environment, University of Delaware, Lewes, DE 19958, USA
e-mail: agartman@udel.edu

G. W. Luther III
e-mail: luther@udel.edu

D. W. Chu
Department of Chemistry and Biochemistry, School of Marine Science and Policy, College of Earth, Ocean and Environment, University of Delaware, Lewes, DE 19958, USA

C. P. Janzen
Department of Chemistry, Susquehanna University, Selingsgrove, PA 17870, USA

E. L. Becker
Biology Department, Penn State University, University Park, PA 16801, USA

R. A. Beinart · P. R. Girguis
Department of Organismic & Evolutionary Biology, Harvard University, Cambridge, MA 02138, USA

Present Address:

S. Ma
Department of Earth and Planetary Science, University of California, Berkeley, CA 94720, USA

Present Address:

M. Yücel
Laboratory of Benthic Ecogeochemistry (LECOB), Observatoire Océanologique de Banyuls, Université Pierre et Marie Curie—Paris 6, 66651 Banyuls-sur-mer, France

May 2009 show either thiosulfate or polysulfides. These in situ data indicate that abiotic sulfide oxidation does not readily occur as H_2S contacts oxic bottom waters. Calculated abiotic potential sulfide oxidation rates are $<10^{-3} \mu\text{M}/\text{min}$ and are consistent with slow oxidation and the observed lack of sulfur oxidation intermediates. It is known that the thermodynamics for the first electron transfer step for sulfide and oxygen during sulfide oxidation in these systems are unfavorable, and that the kinetics for two electron transfers are not rapid. Here, we suggest that different metal catalyzed and/or biotic reaction pathways can readily produce sulfur oxidation intermediates. Via shipboard high-pressure incubation experiments, we show that snails with chemosynthetic endosymbionts do release polysulfides and may be responsible for our field observations of polysulfides.

Keywords Sulfide oxidation · Kinetics · Hydrothermal vents · Diffuse flow · Lau Basin · In situ chemistry

1 Introduction

Sulfide speciation is an integral component of the hydrothermal environment, being relevant for biotic and abiotic processes, and influencing the transport of metals and other hydrothermally emitted species (Hannington et al. 1995; Luther et al. 2001a). At hydrothermal vents, chemosynthetic microorganisms live in diffuse flow hydrothermal vent zones, typically at temperatures ranging above $2\text{--}70^\circ\text{C}$, and make use of the electrons in free hydrogen sulfide ($\sum\text{H}_2\text{S}$ and HS^-) to generate energy for carbon fixation. Thus, they form the basis of primary productivity, obtaining energy from the oxidation of hydrogen sulfide (Eq. 1, Jannasch and Wirsén 1979).



H_2S also reacts with aqueous metal species and precipitates to yield large-scale sulfide deposits. In the presence of O_2 and metals, H_2S may also oxidize to sulfur intermediates and eventually to seawater sulfate. Between sulfide (with a -2 oxidation state on sulfur) and sulfate (with a $+6$ oxidation state), there are a number of sulfur species with intermediate oxidation states, including polysulfides (mix of 0 and -2), elemental sulfur (0), polythionates (0 and $+2$), thiosulfate (-1 and $+5$, 0 and $+4$, or -2 , $+6$) (Vairavamurthy et al. 1993), and sulfite ($+4$).

The formation of polysulfides, elemental sulfur, thiosulfate, sulfite, and polythionates (e.g., tetrathionate) has been demonstrated and characterized in laboratory studies (Chen and Morris 1972; dos Santos Afonso and Stumm 1992; Hoffmann 1977; Yao and Millero 1996). These sulfur intermediates have been observed in several field studies that performed analyses on samples returned to the laboratory (Batina et al. 1992; Ciglenecki and Cosovic 1997; Gun et al. 2000; Hayes et al. 2006; Kamyshny and Ferdelman 2010; Luther et al. 1985; Wang et al. 1998). However, only a few in situ studies have observed these sulfur intermediates (Luther et al. 2001b; Mullaugh et al. 2008; Rozan et al. 2000; Waite et al. 2008).

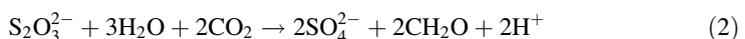
The chemical environments that are available in diffuse hydrothermal flows are known to dictate the distribution of vent fauna (Luther et al. 2001a, b). A number of additional studies over the past 10 years have further contributed to our understanding of how diffuse flow zone chemistry affects megafaunal organism distribution (Le Bris et al. 2003, 2006; Moore et al. 2009; Mullaugh et al. 2008; Nees et al. 2008; Podowski et al. 2009, 2010; Sarrazin et al. 1999; Shank et al. 1998), the variation of diffuse flow zone chemistry in contrast to end-member high temperature chemistry (Scheirer et al. 2006), and the

distribution of organic material and its relationship to metal speciation in diffuse flow zones (Sander et al. 2007, Sarradin et al. 2009). Previous work on hydrothermal sulfur speciation from discrete hydrothermal diffuse flow fluid samples—as well as in the chemoautotrophic tubeworm symbiosis *Riftia pachyptila* by Gru et al. (1998)—used reverse-phase HPLC to characterize sulfide, sulfite, thiosulfate, cysteine, and glutathione. The detection limits of this method are lower than our detection limits for thiosulfate and can additionally measure cysteine and glutathione. However, the number of samples processed is much fewer, and the method is not in situ. Vetter and Fry (1998) also analyzed the sulfur content of molluscs and vestimentiferans, showing that chemoautotrophic symbioses build up elemental sulfur as a result of symbiont sulfide oxidation (Eq. 1).

In situ chemical detection is increasingly recognized as important when considering diffuse flow zones, due to their temporal instability and chemical disequilibrium. In contrast to high temperature vents, which have rapid vertical rates of emission, the vertical flow rates at diffuse flow zones can be faster or slower than lateral current flow. This lateral movement of water contributes to the rapid change (over the course of seconds) in temperature and chemistry that has been observed at Lau Basin at a stationary point (Mullaugh et al. 2008), emphasizing the need to collect in situ data in order to better elucidate the rapidly changing characteristics of diffuse flow zones. Le Bris et al. (2006) compared measured values of sulfide taken in situ and on board ship and found significantly reduced values were recorded on board ship, most likely due to the combined effects of sulfide oxidation and precipitation of FeS.

The ratio of H₂S to temperature in diffuse flow systems, known as the *S/T* ratio, has become a useful indicator of the sulfide content of a particular diffuse flow zone. Le Bris et al. (2006) explored the significance of the *S/T* ratio using an in situ flow analyzer to take sulfide, temperature, and pH measurements to compare the relationship between sulfide, temperature, and macrofaunal habitat in diffuse flow zones at EPR. *S/T* was found to correlate over 3 years for the same habitat type at the same vent site and different habitat types were found to exhibit different *S-to-T* ratios (Le Bris et al. 2006). Nees et al. (2008) also proposed the idea that *S/T* would be characteristic of a vent site and not change on subsequent studies, but found the *S/T* ratio had greatly increased due to eruptions that had occurred at EPR 9°50'N between samplings. Using diffuse flow fluids recovered from the seafloor prior to mixing with ambient seawater, Shank et al. (1998) also observed large increases in emitted sulfide and iron after the eruption at 9°50'N in 1991. It is likely that eruptions modify the network of crustal cracks through which diffuse flow is emitted, changing the characteristics of the particular diffuse flow zone, including the *S/T* relationship.

Previous work on in situ sulfur speciation at Lau Basin has been reported by Waite et al. (2008) who correlated the distribution of thiosulfate and organisms and detected polysulfides based on data collected in June 2005. Mullaugh et al. (2008) also noted the presence of thiosulfate based on data collected in 2006. In both studies, the oxidized species have been found to correlate with the distribution of the mussel *Bathymodiolus brevior* and the red-brown Fe(III) and Mn(III,IV) substrate on which the mussel resides. Waite et al. (2008) suggested that the mussels could metabolize thiosulfate directly as in Eq. 2, but did not have experimental data showing chemosynthesis based on thiosulfate by the mussels.



The in situ data presented herein were collected on cruises to the same four vent sites at Lau Basin in 2006 and 2009. These data demonstrate that there was an increase in observations of oxidized sulfur intermediate products at Lau Basin from 2006 to 2009, and we discuss the relationship between these intermediates and the biological and/or

geological substrate, sulfide, oxygen, and temperature. In addition, we also measured the production of oxidized sulfur compounds from a chemoautotrophic symbioses—the vent snail *Ifremeria nautili*—maintained on board ship in high-pressure respirometry aquaria. These data provide the first direct measure of polysulfide concentrations associated with a hydrothermal vent symbiosis and provide insight into the rate of polysulfide production by these organisms.

2 Materials and Methods

2.1 Study Site

Lau Basin is a back-arc basin located in the southwest Pacific, at approximately 176°W and 21°S, and is located between the Lau ridge on the west and the Tonga ridge on the east (Fig. 1). For this study, we focused on the four most biologically active vent sites that are located north to south along the Eastern Lau Spreading Center/Valu Fa ridge. The Tonga trench, where subduction is occurring, is nearer to the southern sites (40 km) than the northern sites (110 km). This results in a north–south gradient of spreading rate, crustal thickness, and geological substrate. The northern sites are deeper (~2,700 m), are more rapidly spreading (9.7 cm/year), have a thinner crust (~5.5 km), and are basaltic. The southern sites are shallower (~1,900 m), spread more slowly (3.9 cm/year), have greater crustal thickness (~9 km), and are andesitic. The andesitic substrate is more friable and more acidic. Kilo Moana (KM) and Tow Cam (TC) are northern sites, whereas ABE and Tu'i Malila (Tui) are considered southern sites because of geological similarity, even though ABE is geographically closer to the northern sites (Martinez et al. 2006).

Diffuse flow data were collected on a total of twelve dives using the ROV Jason II in 2009. Three dives were performed at KM, two at TC, five at ABE, and two at Tui. These data were

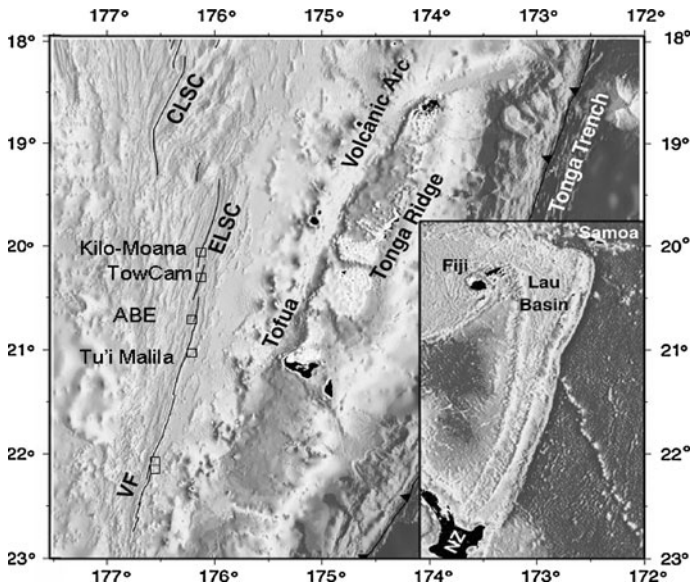


Fig. 1 Map of Lau Basin and the individual study sites. Reproduced with permission from B. Taylor. For further details see Taylor et al. (1996)

collected in the diffuse flow zone. All chemistry data (see below) were taken in diffuse flow areas with a temperature of less than 70°C, mainly on and around areas inhabited by macrofauna. The highest temperature water was observed to be shimmering and free of visible mineral particulates, in contrast to the high temperature, focused flow black smokers.

2.2 Electrochemistry

Voltammetric microelectrodes, as developed by Brendel and Luther (1995) and Luther et al. (2001a, b, 2008) were used for chemical analysis. The methodology is briefly described here. Working electrodes were solid state Au-amalgam, constructed using 100 µm gold wire. The reference electrode was a solid state Ag/AgCl, and the counter electrode was a platinum wire. The electrodes were mounted in conjunction with a thermocouple inside a Delrin wand and manipulated using the ROV Jason II, which also contained the titanium casing with the electronics. Sets of ten cyclic voltammograms were collected by conditioning the electrode at the initial potential (−0.05 V) for 2 s, then scanning from −0.05 to −1.8 V and back to −0.05 V at a scan rate of 2 Vs^{−1}. A conditioning potential at −0.9 V was applied for 5 s before the first scan of each set of ten scans as a way of ensuring a clean electrode surface. Temperature measurements were recorded simultaneously with each electrode scan. Au-amalgam microelectrodes are non-selective and can measure the concentrations in situ of a suite of important redox species simultaneously. The sensor communicated with a laptop on board ship via the Jason II fiber optic cable, and the scans were taken using software from the manufacturer (AIS, Inc). Table 1 provides electrode reactions and detection limits for chemical species identified under the operating conditions used, including dissolved O₂, H₂S (∑H₂S and HS[−]), S₂O₃^{2−}, S_x^{2−} [S(−2) and S(0)]. Figure 2a, b show scans for thiosulfate and polysulfides, respectively. There is no standard for FeS, so the results are reported in current, which is proportional to concentration. Sulfite can be measured as HSO₃[−] (Luther et al. 1985) at pH values <6, which are not common at the vent sites studied, so sulfite is not expected to be detected even if present.

The shape of the current/potential curve is dependent on the type of reaction taking place at the electrode. Sulfide is a quasi-reversible reaction. Many reactions exhibit an S-shaped current/potential curve; however, the sulfide cathodic curve is peak shaped rather than S shaped because of the formation of HgS on the mercury drop. In scanning to negative potential, the removal of sulfide results in a stripping reaction. As described by Rozan et al. (2000), all sulfur species give one peak except for polysulfides. S_x^{2−} exists in two oxidation states [S(−II) and (x − 1)S⁰] and may be fully resolved using scan rates of 1,000 mV s^{−1} or greater, as done in this study (see Fig. 2b).

2.3 Biological and Geological Substrate Characterization

The location where electrochemical scans were taken was characterized by the vent site (north to south), as well as by the immediate biological and/or geological substrate. The substrate correlation was done as described by Podowski et al. (2009, 2010), who used high-definition photomosaic mapping. The majority of scans were taken over hydrothermal vent macrofauna. Scans taken over the most frequently occurring substrates were grouped for analysis. Scans taken over bare rock were labeled “rock”. Scans taken over the mussel *Bathymodiolus brevior* were labeled mussel. Scans taken over the two snail species of interest, *Alviniconcha* spp. and *Ifremeria nautilei*, were grouped separately and labeled *Alviniconcha* and *Ifremeria*. Scans taken over less frequently occurring substrates were grouped together as “other”.

Table 1 Electrode reactions for the chemical species of interest in this study at the Au/Hg electrode versus the saturated calomel electrode (SCE)

		E_p (V)	MDL (μM)
(1a)	$\text{O}_2 + 2\text{H}^+ + 2\text{e}^- \rightarrow \text{H}_2\text{O}_2$	-0.30	5
(1b)	$\text{H}_2\text{O}_2 + 2\text{H}^+ + 2\text{e}^- \rightarrow \text{H}_2\text{O}$	-1.3	5
(2a)	$\text{HS}^- + \text{Hg} \leftrightarrow \text{HgS} + \text{H}^+ + 2\text{e}^-$	Adsorption onto Hg <-0.60	
(2b)	$\text{HgS} + \text{H}^+ + 2\text{e}^- \rightarrow \text{HS}^- + \text{Hg}$	~-0.60	<0.2
(3a)	$\text{Hg} + \text{S}_x^{2-} \leftrightarrow \text{HgS}_x + 2\text{e}^-$	Adsorption onto Hg >-0.60	
(3b)	$\text{HgS}_x + 2\text{e}^- \rightarrow \text{Hg} + \text{S}_x^{2-}$	~-0.60	<0.2
(3c)	$\text{S}_x^{2-} + x\text{H}^+ + (2x - 2)\text{e}^- \rightarrow x\text{HS}^-$	~-0.60	<0.2
(4)	$2\text{S}_2\text{O}_3^{2-} + \text{Hg} \leftrightarrow \text{Hg}(\text{S}_2\text{O}_3)_2^{2-} + 2\text{e}^-$	-0.15	30
(5)	$\text{FeS} + 2\text{e}^- + \text{H}^+ \rightarrow \text{Fe}(\text{Hg}) + \text{HS}^-$	-1.1	Molecular species
(6)	$\text{Fe}^{2+} + \text{Hg} + 2\text{e}^- \leftrightarrow \text{Fe}(\text{Hg})$	-1.43	15
(7)	$\text{Mn}^{2+} + \text{Hg} + 2\text{e}^- \leftrightarrow \text{Mn}(\text{Hg})$	-1.55	10

All data were obtained with a 100- μm diameter electrode ($A = 7.85 \times 10^{-3} \text{ mm}^2$) and were performed using cyclic voltammetry at a scan rate of 2 V/s s^{-1} . Potentials can vary with scan rate and concentration, e.g., on increasing concentration, the sulfide signal becomes more negative. Detection limit can be enhanced with faster scan rates (Bond 1980). For O_2 in the presence of sulfide, the MDL is closer to 10–15 μM

When applying potential from a positive to negative scan direction, sulfide and S(0) react in a two-step process (2a—adsorption onto the Hg surface; 2b—reduction in the HgS film) and polysulfides react in a three-step process (3a—adsorption onto the Hg surface; 3b—reduction in the HgS_x film; 3c—reduction of the S(0) in the polysulfide). Increasing the scan rate separates electrode reactions 3b and 3c into two peaks because Eq. 4c is an irreversible process (increasing scan rate shifts this signal; Bond 1980)

MDL minimum detection limit

2.4 Incubations

All experiments were conducted on board the R/V *Thomas G. Thompson* from May to July 2009. *Ifremeria nautiliei* (Bouchet & Warén, 1991) were collected by the ROV JASON from the ABE vent field (20 45.794323°S, 176 11.466148°W) during dive J2-423 from a depth of 2,152 m. Snails were brought to the surface in a thermally insulated container (Mickel and Childress 1982). After arrival on board ship, the snails most responsive to touch were immediately placed into titanium flow-through, high-pressure respirometer aquaria (as in Henry et al. 2008), where they were maintained in 0.2 micron filter-sterilized flowing seawater for approximately 24 h at 15°C and 27.5 Mpa prior to experimentation.

To simulate the seawater chemistry found in situ, the 0.2-micron filter-sterilized seawater was pumped into an acrylic gas equilibration column and bubbled with carbon dioxide, hydrogen sulfide, oxygen, and nitrogen to achieve the desired dissolved gas concentrations (Girguis and Childress 2006). Seawater from the equilibration column was delivered to the three aquaria by high-pressure pumps (American Lewa, Inc. Holliston, MA USA). High-pressure aquaria were maintained at 15°C in our climate-controlled laboratory, while aquaria pressures were maintained at 27.5 Mpa via diaphragm back pressure valves (StraVal, Inc.). Vessel effluents were directed through a computer-controlled stream-selection valve that diverted one stream to the analytical instrumentation every 30 min so that either the initial water or a chamber with live animals could be analyzed for chemical components. The analytical system consisted of a membrane-inlet quadrupole mass spectrometer to determine all dissolved gas concentrations, an inline oxygen optode

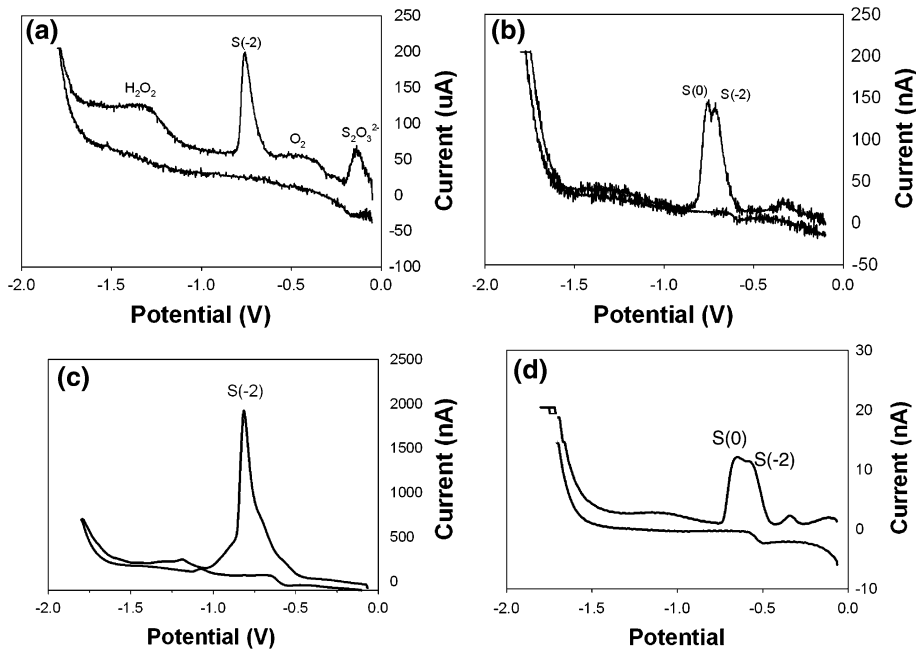


Fig. 2 Representative voltammetric scans. **a** In situ data from TC showing that thiosulfate, hydrogen sulfide, and oxygen can coexist. **b** In situ data from Tui showing $\text{S}(0)$ from polysulfide as well as $\text{S}(-2)$ from sulfide and polysulfide. **c** Data from initial waters fed to the incubation chambers. **d** Data from the waters after passing through the *Ifremeria* chamber showing that $\text{S}(0)$ from polysulfides is released

(Golden Scientific Inc), and an inline pH electrode (Radiometer Inc). In addition to the mass spectrometric analyses, hydrogen sulfide concentrations were determined by a quantitative colorimetric assay (Cline 1969). For this study, a voltammetric flow cell was also added to the inline analytical instrumentation (Luther et al. 2002), so that hydrogen sulfide, polysulfides, thiosulfate, and oxygen could be determined.

For these experiments, *Ifremeria* were placed in the respirometer aquaria and were maintained in conditions typical of those in situ, namely total dissolved inorganic carbon (i.e., $\sum\text{CO}_2$) = 5.5–6 mM, total dissolved sulfide (i.e., $\sum\text{H}_2\text{S}$) = 250 μM , dissolved O_2 = 180 μM , and dissolved NO_3 = 40–50 μM , pH = 6.5, temperature = 15°C, pressure = 27.5 Mpa. *Ifremeria* were maintained in these conditions until “autotrophy”, during which they exhibited a net uptake of dissolved inorganic carbon, oxygen, and sulfide, as well as net elimination of proton equivalents. One aquarium was operated without hosting any organisms and served as our control (for abiotic reactions or those processes mediated by any free-living bacteria). All dissolved initial concentrations, as well as pH and temperature, were held at these “typical” conditions for the duration of the experiment. At the end of each experiment, snails were promptly removed, weighed on a motion-compensated shipboard balance, dissected, and frozen in liquid nitrogen for other analyses.

3 Results

3.1 Sulfide, Temperature, and Oxygen from 2006 to 2009

In order to address temporal change at the diffuse flow vent sites, we compare the free sulfide ($\sum \text{H}_2\text{S}$ and HS^-) to temperature (S/T) ratios for each site (Table 2). Each of the 11,000 scans was considered individually. Sulfide and oxygen were present in most of the scans, but not all. Eighty-three percent of scans contained detectable oxygen, while ninety percent of scans contained detectable sulfide. The S/T ratio at each site will result from a combination of factors, including the concentration of sulfide in the original fluid, sub-seafloor mixing, and water/rock interactions. The S/T value used here is the slope that is obtained when all the sulfide data collected at each site are plotted against the corresponding temperature data (Fig. 6a). At Lau Basin, the four major sites measured exhibit a change in the sulfide to temperature ratio from 2006 to 2009 that is greater than the error of the slope (Table 2). For the three northern sites, the S/T ratio increased. However, in both years, the S/T ratios follow the same pattern, decreasing from north to south. At the southernmost site, Tu'i Malila, S/T varies by less than ten percent from year to year. By contrast, the average sulfide measured nearly doubled at the three northernmost sites, although the S/T did not change so drastically. The characteristic decrease in S/T ratio from north to south is a reflection of the change from the two northern sites (KM and TC), which are basalt hosted and further from the subduction zone, to the two southern sites (ABE and Tui), which are shallower, nearer to the subduction zone, and with a greater proportion of andesite in the host rock. Mottl et al. (2011) have noted a similar decrease in S/T from north to south for focused flow hydrothermal vents ($>300^\circ\text{C}$), whereas Podowski et al. (2010) noted this trend in the diffuse flow zone in 2006.

Table 2 Lau Basin average oxygen, sulfide, and temperature data with 95% confidence intervals

Lau Basin average sulfide and temperature ratios, north to south								
2006				2009				
Avg O ₂	Avg H ₂ S	Avg T	S/T		S/T	Avg T	Avg H ₂ S	Avg O ₂
90 ± 1.8	13 ± 0.94	4.5 ± 0.15	5.6 ± 0.07	KM	7.0 ± 0.09	5.7 ± 0.16	23 ± 1.4	92 ± 1.8
78 ± 2.1	16 ± 1.3	4.7 ± 0.24	4.2 ± 0.09	TC	4.9 ± 0.09	7.2 ± 0.34	25 ± 1.8	80 ± 2.6
116 ± 2.3	9.0 ± 0.79	5.4 ± 0.20	2.7 ± 0.06	ABE	4.7 ± 0.07	7.2 ± 0.25	17 ± 1.6	77 ± 1.7
77 ± 2.0	14 ± 1.1	9.1 ± 0.43	2.1 ± 0.04	Tui	1.9 ± 0.03	8.2 ± 0.40	13 ± 1.1	75 ± 2.4
			Median T		Median H ₂ S			
			KM	3.5	5.7	104		
			TC	4.5	9.5	92		
			ABE	4.0	2.6	83		
			Tui	5.0	4.2	87		

S/T is the slope of all sulfide data plotted against all temperature data for that site. H₂S and O₂ concentrations are given in μM . T is in $^\circ\text{C}$. Median data are also given for 2009

KM Kilo Moana, TC Tow Cam, Tui Tu'i Malila

3.2 Sulfide Oxidation Considerations

Due to the presence of H₂S and O₂ in the waters studied, some sulfide oxidation products may be expected. However, as shown below, only 5% of all measurements taken contain sulfur oxidation intermediates. Figure 3a shows the thermodynamics for the reactions of H₂S with O₂ and other reactive oxygen species (ROS) where each half reaction is a one-electron transfer step (Luther 2010). The only one-electron reactant that can effectively oxidize H₂S is OH·, as HS· and O₂⁻ are not favorable products for O₂ oxidation (Eq. 3).



Sulfide oxidation by O₂ occurs in the presence of Fe²⁺ that can react with O₂ to form O₂⁻ and H₂O₂. Because O₂ leads to H₂O₂ stoichiometrically via Fe²⁺ catalysis, the rate of sulfide oxidation is still first order with respect to both O₂ and H₂S (Eq. 4). Thus, Fe²⁺ is a catalyst that leads to ROS that can oxidize H₂S (Luther 2010, Vazquez et al., 1989, Fig. 3b). The two-electron transfer reactions of ROS to react with H₂S to form S(0) and eventually S₈ (Fig. 3b) are favorable but the reaction with O₂ is kinetically slow because of the partially occupied orbitals for O₂ (Luther 2010, Luther et al. 2011). H₂O₂ has no kinetic barrier to reaction with sulfide (Eq. 5, Luther et al. 1998; Luther 2010).



Because the formation of the HS· radical is not favorable, H₂S oxidation should proceed through the formation of S⁰ atoms that can then react with either H₂S or HS⁻ to form polysulfides, S_x²⁻ (Eq. 6).

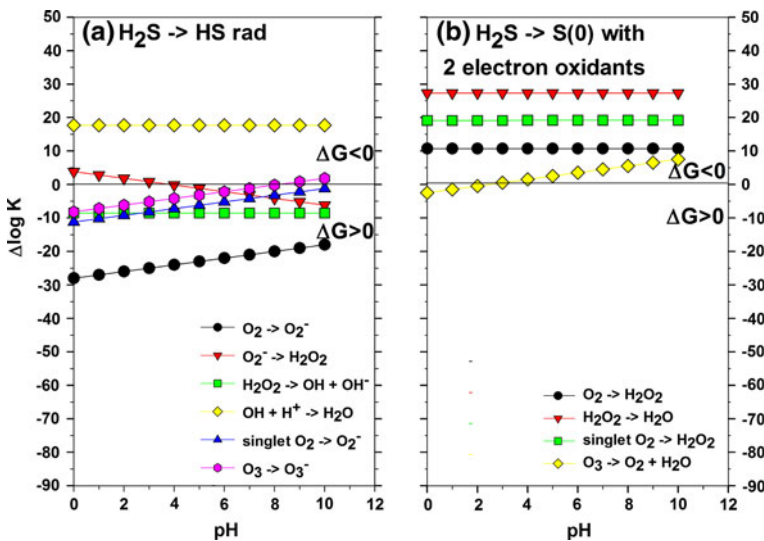
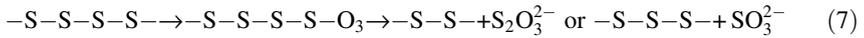


Fig. 3 a The one-electron transfer reactions of H₂S with oxygen species to form HS⁻ (b). The two-electron transfer reactions of oxygen species to react with H₂S to form S(0). A positive Δlog K on the y-axis indicates a favorable reaction and a negative Δlog K indicates an unfavorable reaction as ΔG₀ = - RT ln K = - 2.303RT log K. Calculations performed using the thermodynamic data (at 25°C and 1 atm) tabulated by Maloy (1985), Stumm and Morgan (1996) and Stanbury (1989)



This can occur until S_9^{2-} forms, which decomposes to S_8 and HS^- . Polysulfides are highly reactive and do not persist or build up to significant concentrations in oxygenated waters. They are most stable at near neutral pH (Chen and Gupta 1973) and oxidize approximately four times faster than sulfide (Kleinjan et al. 2005). The terminal S atom of S_x^{2-} can also be oxidized to sulfite and thiosulfate as below (Eq. 7).



Thiosulfate is a metastable intermediate in solution and tends toward stability so much that it has been described as an end product of sulfide oxidation (O' Brien and Birkner 1977). O' Brien and Birkner (1977) observed little $\text{S}_2\text{O}_3^{2-}$ oxidation to occur over the course of 3 days, at pH values between 4 and 10. The oxidation products of polysulfides are pH dependent, and thiosulfate becomes the primary oxidation product at pH values greater than 8.5. Increases in the concentration of thiosulfate may be due to a rise in pH; however, the pH values at our site are around 7 and do not approach the pH values where thiosulfate dominates as an oxidation product in laboratory studies (Chen and Morris 1972; Chen and Gupta 1973). Based on the thermodynamic and chemical speciation considerations discussed above, we present the following analysis of the in situ data.

3.3 Thiosulfate, 2006 to 2009

Thiosulfate followed no discernible pattern between vent sites from 2006 to 2009. In 2009, thiosulfate ranged in concentration from the detection limit to approximately 450 μM . In 2006, the northernmost site (Kilo Moana) and the southernmost site (Tu'i Malila) had the highest number of scans in which thiosulfate was detected (Fig. 4a). In 2009, we observed the most incidences of thiosulfate at Kilo Moana, but in contrast, we observed no thiosulfate at Tu'i Malila. It is also apparent that a higher percentage of scans contained thiosulfate in 2009 ($\sim 5\%$, 529 scans) than in 2006 ($<1\%$, 66 scans) (Fig. 4a). Tow Cam is the only site where the relative number of thiosulfate scans is similar from 2006 to 2009.

The increased incidences of thiosulfate over all sites from 2006 to 2009 may partially be explained by the increased overall H_2S detected in diffuse flow zones (Table 2). The greater concentration of sulfide can result in a greater concentration of oxidized sulfur species, assuming the oxidizing capacity of the oceanic waters was similar in the 2 years studied. The average oxygen detected was similar at three of the four sites from 2006 to 2009 (Table 2) suggesting no significant change in the oxidizing capacity of the waters over this time period. In fact, we see no relationship between the concentration of oxygen or the oxygen to temperature ratio versus the concentration of any oxidized sulfur species detected (data not shown).

To better understand potential sulfide oxidation in the current dataset, we applied the overall rate equation for the oxidation of H_2S shown in Eq. 8 (Millero 1986). It is first order with respect to oxygen and sulfide, and the rate constant (k) is independent of the original concentration of sulfide. This rate equation was developed using seawater, where the effects of metal catalysis were considered to be low.

$$-d[\text{H}_2\text{S}]/dt = k[\text{H}_2\text{S}][\text{O}_2] \quad (8)$$

Using the average concentration of sulfide, oxygen, and the average temperature from Lau Basin in 2006 and 2009, we determined the potential rate of sulfide oxidation

Fig. 4 **a** Comparison of thiosulfate at Lau Basin, 2006–2009. The y-axis shows the percent of total scans taken that contained thiosulfate, for each site: Kilo Moana (KM) Tow Cam (TC) ABE and Tu'i Malila (Tui). **b** Percent of scans at each site that contained polysulfides **(c)**. Percent of scans at each site that contained "aqueous metals, including FeS, Fe²⁺ and Mn²⁺" species

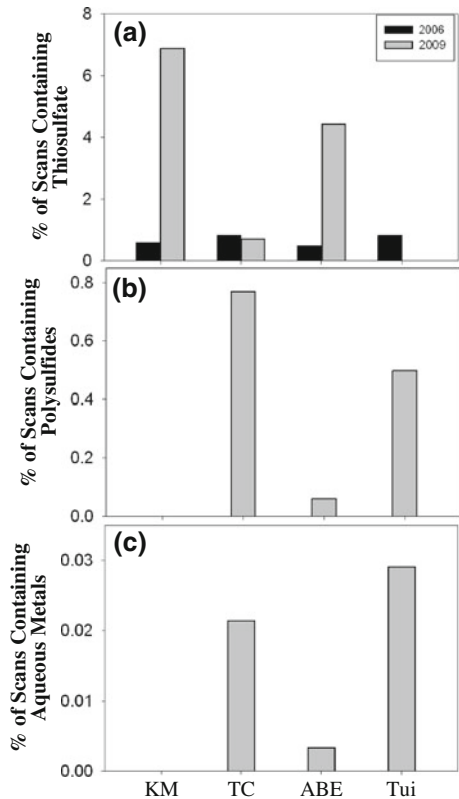


(Table 3) for each site, for each year, after calculating the rate constant based on Eq. 9 (Millero et al. 1987). Using median values would result in a slightly decreased rate. An average ionic strength of 0.7 was assumed for all sites, and calculations were done for pH values of 6, 7, and 8. The rate of oxidation increases by about 50% from pH 6 to 7 and another 50% from pH 7 to 8, but the amount of sulfide oxidation is well below our detection limits given in Table 1.

$$\log k = 10.5 + 0.16\text{pH} - 3 \times 10^3 T^{-1} + 0.49I^{1/2} \quad (9)$$

These calculated rates are based on seawater that was not obtained by trace metal clean methods and with no added trace metals. When trace metals are added, the rate will increase 20-fold (Luther et al. 2011; Pyzik and Sommer 1981; Vazquez et al. 1989). For chemosynthetic oxidation of sulfide, the rate will increase by 1,000-fold as shown by Luther et al. (2011) and in the incubation experiments below.

As shown in Table 3, H₂S, T, and the potential rate of oxidation increased from 2006 to 2009 for KM, TC, and ABE, and decreased at Tui, corresponding with our data that the oxidized products at Tui decreased from 2006 to 2009, while increasing at KM and ABE (Fig. 4). However, calculated oxidation rates at TC increased by more than two fold from 2006 to 2009, while observed incidences of thiosulfate exhibited very little change. Despite this, the highest number of incidences of polysulfides per site was detected at TC in 2009

Table 3 The calculated abiotic sulfide oxidation rates at Lau Basin from 2006 to 2009, using average temperature, sulfide, and oxygen data and Eq. 8

	Lau Basin					
	2006			2009		
	pH 6	pH 7	pH 8	pH 6	pH 7	pH 8
Kilo Moana						
Log <i>k</i>	1.02	1.18	1.34	1.07	1.23	1.39
Rate	2.03E-04	2.93E-04	4.24E-04	4.18E-04	6.05E-04	8.74E-04
Tow Cam						
Log <i>k</i>	1.03	1.19	1.35	1.13	1.29	1.45
Rate	2.15E-04	3.11E-04	4.50E-04	4.44E-04	6.42E-04	9.27E-04
ABE						
Log <i>k</i>	1.06	1.22	1.38	1.13	1.29	1.45
Rate	2.03E-04	2.94E-04	4.25E-04	2.96E-04	4.29E-04	6.19E-04
Tui Malila						
Log <i>k</i>	1.20	1.36	1.52	1.17	1.33	1.49
Rate	2.94E-04	4.25E-04	6.15E-04	2.30E-04	3.32E-04	4.80E-04
Incubation experiments						
Actual biotic rate	Calculated abiotic rate		Initial H ₂ S	Initial O ₂	<i>T</i>	
27.83	2.90E-02		312	180	15	

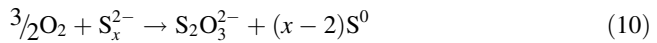
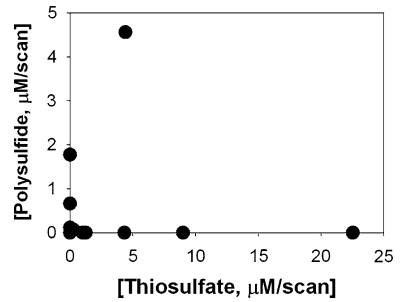
Log *k* was calculated according to Eq. 9 (Millero et al. 1987). All concentrations are in μM , *T* is in $^{\circ}\text{C}$, and rate is in $\mu\text{mol L}^{-1} \text{min}^{-1}$

(Fig. 4b). Due to the relatively slow oxidation of sulfide calculated and the low percentage of oxidized sulfide species detected at or just above the substrate, we conclude that the majority of sulfide may be oxidized elsewhere in the water column, where it can also be used by free-living bacteria. However, even at 1 meter above the substrate, the flow rate in diffuse flow areas is so rapid that no sulfide oxidation intermediates would be easily detected with the detection limits of our method.

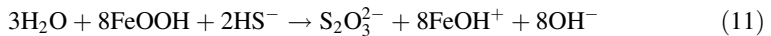
3.4 Polysulfides and other species, 2009

Here, we address polysulfides and the aqueous iron species FeS and Fe²⁺ detected at Lau Basin in 2009 and compare these species to thiosulfate. Polysulfide concentrations (as S(0), Table 1, Eq. 3c) detected in 2009 ranged from the detection limit to approximately 400 μM . The trends observed in partially oxidized sulfur species in 2009 are shown in Figs. 4b, c and 5. Figure 4 shows the percent of scans at each site containing each species, from north to south. Both polysulfides and thiosulfate tend to increase with increasing *S*/*T* ratio. This trend is expected based on the rates calculated in Table 3, because as more H₂S is emitted, more H₂S is available to be oxidized. Interestingly, the sites at which thiosulfate was found were almost mutually exclusive from those at which polysulfides were found (Fig. 5). We know that polysulfides are one possible precursor to thiosulfate, as polysulfides react with O₂ according to Eq. 10.

Fig. 5 Concentration of polysulfides versus thiosulfate for each dive. Instances of thiosulfate and polysulfides were mutually exclusive to each other, with one exception



As suggested from 2006 data (Mullaugh et al. 2008) and similar to laboratory studies on the dissolution of iron oxyhydroxides by H_2S (dos Santos Afonso and Stumm 1992, Pyzik and Sommer 1981), the formation of thiosulfate can also be a surface-controlled reaction, taking place on oxidized iron and manganese minerals. The thiosulfate may become an aqueous species after formation on and subsequent desorption from the mineral surface (Eq. 11), providing an explanation for why polysulfides were not found in solutions containing thiosulfate. Additionally, as stated above, the detection limits for polysulfides are quite low ($<0.2 \mu\text{M}$), whereas detection limits for thiosulfate are much higher ($\sim 30 \mu\text{M}$), so thiosulfate may be present in concentrations below our detection limit at some sites where it was not detected.

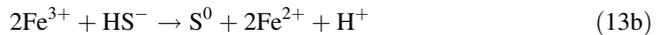
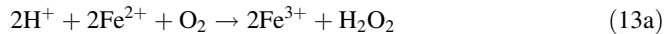


Although thiosulfate can form from precursor polysulfides in the presence of O_2 (Eq. 10), there are other loss pathways for polysulfides. Plotting incidences where FeS_{aq} , Fe^{2+} , and Mn^{2+} were detected reveals a possible sink for the polysulfides that were detected in solution (we note that Fe(II) and Mn(II) , when detected, ranged between the detection limit and $20 \mu\text{M}$). All of the metal ion and FeS_{aq} species are summed as one contribution, “aqueous metal species”, in Fig. 4c, and are plotted vs site along with thiosulfate and polysulfides in Fig. 4a and b, respectively. All three plots are percent of scans taken at each site containing each respective species. In comparing all three plots of Fig. 4, it can be seen that the relative values for polysulfides and other chemical species are lower when values for thiosulfate are high (at KM and ABE) and values for polysulfides and other species are higher when thiosulfate is low (TC and Tui). It is also apparent that dissolved metal containing species are higher in concentration at sites where concentrations of polysulfides are present and lower in concentration at sites with thiosulfate. Chadwell et al. (2001) found that M^{2+} in solution could complex polysulfides, but at higher metal concentrations could result in metal sulfide and elemental sulfur formation, as shown in Eq. 12, which we suggest as a possible loss pathway for polysulfides.



An alternative explanation for the co-occurrence of polysulfides and reduced metal species is the formation pathway presented in equation sequence 13a–c. The reduced metal species detected in solution may become oxidized and can in turn oxidize HS^- in solution, leading to the formation of polysulfides and their decomposition products including elemental sulfur and thiosulfate. The thermodynamics of this sequence is favorable where

Fe^{3+} forms nanoparticles (Luther 2010). Even at low Fe^{2+} concentrations (see Vazquez et al., 1989), Eqs. 13a–c would lead to the rate dependence shown in Eqs. 8 and 9.



3.5 Substrate and oxidized sulfur species

Figure 6a shows the data points used to calculate the S/T ratio for each substrate, while Fig. 6b shows the substrate specific S/T ratio from north to south. The relationship between S/T and substrate (Fig. 6b) reveals that the sites inhabited by *Alviniconcha* exhibit the greatest change in S/T from north to south, with the highest S/T ratio at KM and the lowest S/T ratio at Tui. By contrast, the other snail species of interest, *Ifremeria* consistently inhabit locations with lower than average S/T , indicating a preference for lower sulfide and greater oxygen conditions, as was demonstrated in a previous study (Podowski et al. 2009). Measurements taken over rock were similar to the average at TC and Tui and higher than average at KM and ABE, while measurements taken over Mussel were similar to the average at KM and Tui and lower than average at TC and ABE.

In 2006, polysulfides, one of the precursors to thiosulfate, were not readily detected despite the high sensitivity and excellent detection limits for polysulfides. Data from 2009 suggest that areas with the highest incidences of thiosulfate were found at sites either with a rocky substrate [5% of scans on a rocky substrate contained thiosulfate (223 scans)], with sites containing mussels [5% of scans over mussels contained thiosulfate (85 scans)] or with sites occupied by *Ifremeria* [7% of scans taken over *Ifremeria* contained thiosulfate (125 scans)]. The relationship between these substrates and the oxidized products is not a result of high sulfide concentration, since locations with a rocky substrate have an S/T ratio that was close to the average of all sites. Locations containing mussels had an S/T that was less than or equal to the average of all sites, and locations containing *Ifremeria* had a lower than average S/T ratio (Fig. 6a,b).

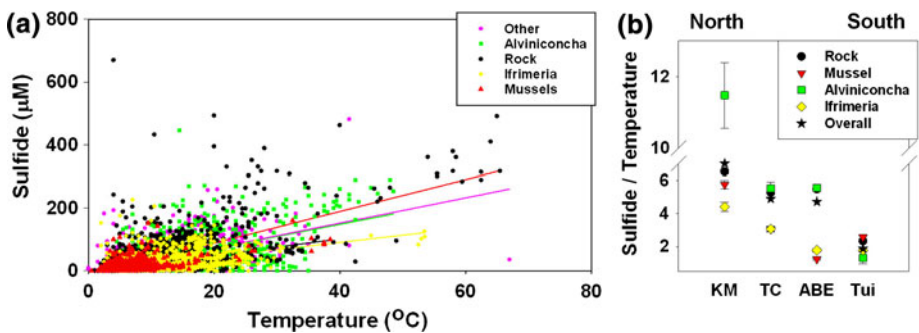


Fig. 6 a Sulfide to temperature plotted for different substrates, for all sites. Actual data points are shown. b S/T ratios for different substrates, correlated with site north to south. KM (Kilo Moana) TC (Tow Cam) ABE, and Tui (Tu'i Malila). Error of the slope is included

Despite the basalt–andesite gradient at Lau Basin and the corresponding north–south trend in S/T ratios, we do not see a north to south relationship between the concentration or occurrence of oxidized species, either in 2006 or in 2009. In 2009, polysulfides were detected mainly over *Alviniconcha* [0.8% of scans over *Alviniconcha* contained polysulfides (5 scans)], rock [0.2% of scans over rock contained polysulfides (7 scans)], and *Ifremeria* [0.2% of scans over *Ifremeria* contained polysulfides (4 scans)]. A total of 31 scans contained polysulfides in 2009 indicating that these are not prevalent due to their reactivity.

Results from 2006 noted that the highest incidences of thiosulfate were located directly above oxidized geological substrate, and in 2009, the co-occurrence of aqueous iron sulfide and polysulfides was observed. Together, these results indicate that the presence or absence of oxidized sulfur species is influenced more by the localized biological or geological substrate, rather than the basalt/andesite distinction.

Previous, but less extensive in situ work at the East Pacific Rise (EPR) had identified polysulfides, but not thiosulfate (Luther et al. 2001b). Lower oxygen concentrations and uniform basaltic substrate at the East Pacific Rise suggest that it is a more reducing environment, which inhibits the fast formation of oxidized sulfur species. Although oxygen is not a direct one-electron abiotic oxidant of sulfide (Fig. 3a) and kinetically a slow two-electron oxidant, higher concentrations of oxygen can result in a more oxidizing environment yielding higher concentrations of soluble and solid Fe(III) and Mn(III,IV) phases, which could potentially catalyze sulfide oxidation. However, we see no relationship between the oxygen detected at a site and the presence of partially oxidized sulfur species.

3.6 Shipboard High-Pressure Incubations Demonstrate Biotic Oxidation to Polysulfides

Another possible interpretation of the location of polysulfides over the two species of snails is that a small subset of the organisms are releasing polysulfides during chemosynthesis (Eqs. 1, 4–6). Pressurized incubations containing the species described in this paper suggest that *Ifremeria* are releasing polysulfides while chemoautotrophic (Fig. 2c,d), in agreement with the highest incidences of polysulfide S(0) observed here (Figs. 2d, 7). Oxidation rates calculated from the loss of sulfide in incubation chambers reveal that biotic sulfide oxidation occurs a thousand times faster in chambers containing *Ifremeria* than would be suggested from abiotic oxidation rates (Table 3). Because the formation of S_x^{2-} is not predicted at such high concentrations by abiotic calculations (Eqs. 8, 9) and because polysulfides are not found downstream in control experiments that contain no organisms, we suggest that the snail's symbionts are responsible for the observed polysulfides. Notably, we are unable to discern whether the observed oxidation was the result of the hosts' sulfide detoxification mechanisms (Arp et al. 1995), the symbionts' metabolic activities, free-living microbes associated with the shell, or abiotic reactions due to metal precipitation on the shell. Future experiments should aim to discern which of these factors most contributes to the observed sulfide oxidation. While Table 3 shows that *Ifremeria* were incubated at higher H_2S and O_2 than is typically encountered in situ, these conditions are well within the large chemical and temperature variations that occur in the diffuse flows. The reason S_x^{2-} was uniformly detected downstream from the *Ifremeria* in incubations, but only periodically in the field remains to be explored. However, the higher sustained concentrations of H_2S and O_2 may have contributed to this effect. No thiosulfate was detected in any of these incubations.

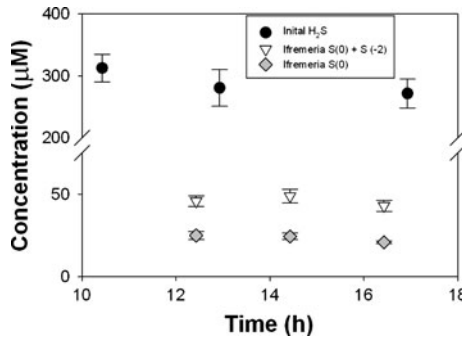


Fig. 7 High-pressure incubation study with *Ifremeria*. The filled circle data points indicate the initial time and subsequent control times that the sterilized equilibration chamber contents with H₂S, O₂, and CO₂ were diverted to the analytical system. The average concentration of each chemical component and standard deviation are given for the 30-min analytical period ($N \geq 25$ for each concentration)

4 Conclusions

Detailed analysis of in situ electrochemical scans taken in the diffuse flow zone of Lau Basin in 2009 reveals increased concentrations of sulfide, and increased occurrences of partially oxidized sulfur intermediates than a similar set of scans taken in the same locations in 2006. The increases in sulfide and temperature, which were observed at the northernmost three sites between 2006 and 2009, may have contributed to the increased concentration of oxidized sulfur species that occurred during the same time period, as shown by calculations of potential oxidation rates in Table 3. However, greater than ninety-four percent of scans taken in 2009, and greater than ninety-nine percent of scans taken in 2006, contained no oxidized sulfur species. This indicates that in the diffuse flow environments sampled, centimeters away from biological and geological substrates, little sulfide oxidation occurs. This is in agreement with the unfavorable thermodynamics for the one-electron transfer reaction between sulfide and O₂ (Fig. 3a) and the slow kinetics for the favorable two-electron transfer (Eqs. 8, 9). While no trend is seen between oxygen concentrations and oxidized sulfur species, or along the north–south gradient, there is an apparent relationship between vent sites (Fig. 4) with each type of oxidized sulfur species. This trend indicates the possibility of different metal-catalyzed pathways (trace metal catalyzed and solid phase oxide) as oxidative loss pathways for hydrothermally generated sulfide in diffuse flow zones. Additionally, we note that the location of in situ data for polysulfides corresponds with incubation results showing the presence of polysulfides downstream from *Ifremeria*, suggesting that the polysulfides detected in the field may be produced and released (under some circumstances) from microbes, symbiotic, or otherwise. Overall, the combination of in situ electrochemical scans along with the calculated abiotic rates of oxidation suggest that the majority of sulfide in the diffuse flow zone is not rapidly oxidized as it reaches oxygenated waters and that sulfide may be most rapidly oxidized by free-living bacteria, symbiotic bacteria, or elsewhere in the water column where metals may play a role in facilitating the abiotic rates of oxidation.

Acknowledgments This paper is submitted in the memory and honor of John W. Morse who made significant contributions to geochemistry and oceanography including the founding of *Aquatic Geochemistry* (Mackenzie et al. 2010). This work was supported by grants from the US National Science Foundation (OCE-0732439 to GWL, OCE-0732369 to PRG, OCE-0732333 to Charles R. Fisher), via the Ridge 2000

program. None of this work would have been possible without the expertise and patience of the ROV JASON II and the R/V Melville crews in 2006, and the ROV JASON II, and the R/V Thomas G. Thompson crews in 2009. We thank Arunima Sen for her assistance with the substrate data. Special thanks to Dr. Charles R. Fisher for his skills as chief scientist and for facilitating data collection.

References

- Arp AJ, Menon JG, Julian D (1995) Multiple mechanisms provide tolerance to environmental sulfide in *Urechis caupo*. *Am Zool* 35:132–144
- Batina N, Ciglenecki I, Cosovic B (1992) Determination of elemental sulphur, sulphide and their mixtures in electrolyte solutions by a.c. voltammetry. *Anal Chim Acta* 267:157–164
- Bouchet P, Warén A (1991) *Ipremeria nautilei*, a new gastropod from hydrothermal vents, probably associated with symbiotic bacteria. *C. R. ACAD. SCI. PARIS, SER. III* 312(10):495–501
- Brendel, PJ, Luther GW III (1995) Development of a gold amalgam voltammetry microelectrode for the determination of dissolved Fe, Mn, O₂, and S(-II) in porewaters of marine and freshwater sediments. *Environ Sci Technol* 29:751–761
- Chadwell SJ, Rickard D, Luther GW III (2001) Electrochemical evidence for metal polysulfide complexes: tetrasulfide (S₄²⁻) reactions with Mn²⁺, Fe²⁺, Co²⁺, Ni²⁺, Cu²⁺, and Zn²⁺. *Electroanalysis* 13:21–29
- Chen KY, Gupta SK (1973) Formation of polysulfides in aqueous solution. *Environ Lett* 4(3):187–200
- Chen KY, Morris JC (1972) Kinetics of Oxidation of Aqueous Sulfide by O₂. *Environ Sci Technol* 6:529–537
- Ciglenecki I, Cosović B (1997) Electrochemical determination of thiosulphate in seawater in the presence of elemental sulphur and sulphide. *Electroanalysis* 9(10):1–7
- Cline JD (1969) Spectrophotometric determination of hydrogen sulfide in natural waters. *Limnol Oceanogr* 14:454–458
- dos Santos Afonso M, Stumm W (1992) Reductive dissolution of Iron(III) (Hydr)oxides by hydrogen sulfide. *Langmuir* 8:1671–1675
- Girguis PR, Childress JJ (2006) Metabolite uptake, stoichiometry and chemoautotrophic function of the hydrothermal vent tubeworm *Riftia pachyptila*: Responses to environmental variations in substrate concentrations and temperature. *J Exp Biol* 209(18):3516–3528
- Gru C, Sarradin PM, Legoff H, Narcon S, Caprais JC, Lallier FH (1998) Determination of reduced sulfur compounds by high-performance liquid chromatography in hydrothermal seawater and body fluids from *Riftia pachyptila*. *Analyst* 123:1289–1293
- Gun J, Goifman A, Shkrob I, Kamyshny A, Ginzburg B, Hadas O, Dor I, Modstov AD, Lev O (2000) Formation of Polysulfides in an oxygen rich freshwater lake and their role in the production of volatile sulfur compounds in aquatic systems. *Environ Sci Technol* 34:4741–4746
- Hannington MD, Jonasson IR, Herzig PM, Petersen S (1995) Physical and chemical processes of seafloor mineralization at mid-ocean ridges, pp 115–157. In: Humphris SE, Zierenberg RA, Mullineaux LS, Thomson RE (eds) Seafloor hydrothermal systems: physical, chemical, biological, and geological interactions. Geophysical monograph 91. American Geophysical Union, Washington, DC
- Hayes MK, Taylor GT, Astor Y, Scranton MI (2006) Vertical distributions of thiosulfate and sulfite in the Caraiço Basin. *Limnol Oceanogr* 51(1):280–287
- Henry MS, Childress JJ, Figueroa D (2008) Metabolic rates and thermal tolerances of chemoautotrophic symbioses from Lau Basin hydrothermal vents and their implications for species distributions, Deep Sea Research Part I: Oceanographic Research Papers 55(5):679–695
- Hoffmann MR (1977) Kinetics and mechanism of oxidation of hydrogen sulfide by hydrogen peroxide in acidic solution. *Environ Sci Technol* 11:61–66
- Jannasch HW, Wirsén CO (1979) Chemosynthetic primary production at East Pacific Sea Floor spreading centers. *Bioscience* 29:592–598
- Kamyshny A Jr, Ferdelman TG (2010) Dynamics of zero-valent sulfur species including polysulfides at seep sites on intertidal sand flats (Wadden Sea, North Sea). *Mar Chem* 121:17–26
- Kleinjan WE, de Keizer A, Janssen AJH (2005) Kinetics of the chemical oxidation of polysulfide anions in aqueous solution. *Water Res* 39:4093–4100
- Le Bris N, Sarradin PM, Caprais JC (2003) Contrasted sulphide chemistries in the environment of 13°N EPR vent fauna. *Deep-Sea Res I* 50:737–747
- Le Bris N, Rodier P, Sarradin PM, Le Gall C (2006) Is temperature a good proxy for sulfide in hydrothermal vent habitats? *Cah Biol Mar* 47:465–470

- Luther GW III (2010) The role of one- and two-electron transfer reactions in forming thermodynamically unstable intermediates as barriers in multi- electron redox reactions. *Aquat Geochem* 16:395–420
- Luther GW III, Bono A, Taillefert M, Cary SC (2002) A continuous flow electrochemical cell for analysis of chemical species and ions at high pressure: laboratory, shipboard and hydrothermal vent results. In: Taillefert M, Rozan T (eds) *Environmental electrochemistry: analyses of trace element biogeochemistry*. American Chemical Society Symposium Series; American Chemical Society, Washington, D. C., Chap 4, vol 811, pp 54–73
- Luther GW III, Giblin AE, Varsolona R (1985) Polarographic analysis of sulfur species in marine porewaters. *Limnol Oceanogr* 30(4):727–736
- Luther GW III, Brendel PJ, Lewis BL, Sundby B, Lefrançois L, Silverberg N, Nuzzio DB (1998) Simultaneous measurement of O₂, Mn, Fe, I⁻, and S(-II) in marine pore waters with a solid-state voltammetric microelectrode. *Limnol Oceanogr* 43(2):325–333
- Luther GW III, Rozan TF, Taillefert M, Nuzzio DB, Di Meo C, Shank TM, Lutz RA, Cary SC (2001a) Chemical speciation drives hydrothermal vent ecology. *Nature* 410:813–816
- Luther GW III, Glazer BT, Hohmann L, Popp JI, Taillefert M, Rozan TF, Brendel PJ, Theberge SM, Nuzzio DB (2001b) Sulfur speciation monitored in situ with solid state gold amalgam voltammetric microelectrodes: polysulfides as a special case in sediments, microbial mats and hydrothermal vent waters. *J Environ Monit* 3:61–66
- Luther GW III, Glazer BT, Ma S, Trouwborst RE, Moore TS, Metzger E, Kraiya C, Waite TJ, Druschel G, Sundby B, Taillefert M, Nuzzio DB, Shank TM, Lewis BL, Brendel PJ (2008) Use of voltammetric solid-state (micro)electrodes for studying biogeochemical processes: Laboratory measurements to real time measurements with an in situ electrochemical analyzer (ISEA). *Mar Chem* 108:221–235
- Luther GW, Findlay AJ, MacDonald DJ, Owings SM, Hanson TE, Beinart RA, Girguis PR (2011) Thermodynamics and Kinetics of sulfide oxidation by oxygen: a look at inorganically controlled reactions and biologically mediated processes in the environment. *Front Microbiol Physiol* 62:1–9
- Mackenzie FT, Mucci A, Luther GW III (2010) In Memoriam: John W. Morse (1946–2009) Texas A&M University. *Aquat Geochem* 16:219–221
- Maloy JT (1985) Nitrogen chemistry. In: Bard AJ, Parsons R, Jordan J (eds) *Standard potentials in aqueous solution*, 1st edn. M. Dekker, New York, pp 127–139
- Martinez F, Taylor B, Baker ET, Resing JA, Walker SL (2006) Opposing trends in crustal thickness and spreading rate along the back-arc Eastern Lau Spreading Center: implications for controls on ridge morphology, faulting, and hydrothermal activity. *Earth Planet Sci Lett* 245:655–672
- Mickel TJ, Childress JJ (1982) Effects of pressure and temperature on the EKG and heart rate of the hydrothermal vent crab *Bythograea thermydron* (Brachyura). *Biol Bull* 162:70–82
- Millero FJ (1986) The thermodynamics and kinetics of the hydrogen sulfide system in natural waters. *Mar Chem* 18:121–147
- Millero FJ, Hubinger S, Fernandez M, Garnett S (1987) Oxidation of H₂S in seawater as a function of temperature, pH, and ionic strength. *Environ Sci Technol* 21:439–443
- Moore TS, Shank TM, Nuzzio DB, Luther GW III (2009) Time-series chemical and temperature habitat characterization of diffuse flow hydrothermal sites at 9°50'N East Pacific Rise. *Deep Sea Res II* 56:1616–1621
- Mottl MJ, Seewald JS, Wheat CG, Tivey MK, Michael PJ, Proskurowski G, McCollom TM et al (2011) Chemistry of hot springs along the Eastern Lau Spreading Center. *Geochim Cosmochim Acta* 75(4):1013–1038
- Mullaugh KM, Luther GW III, Ma S, Moore TS, Yücel M, Becker EL, Podowski EL, Fisher CR, Trouwborst RE, Pierson BK (2008) Voltammetric (Micro) electrodes for the in situ study of Fe²⁺ oxidation kinetics in hot springs and S₂O₃²⁻ production at hydrothermal vents. *Electroanalysis* 20(3):280–290
- Nees HA, Moore TS, Mullaugh KM, Holyoke RR, Janzen CP, Ma S, Metzger E, Waite TJ, Yücel M, Lutz RA, Shank TM, Vetrani C, Nuzzio DB, Luther GW III (2008) Hydrothermal vent mussel habitat chemistry, pre- and post- eruption at 9°50' north on the East Pacific Rise. *J Shellfish Res* 27(1):169–175
- O' Brien DJ, Birkner FB (1977) Kinetics of oxygenation of reduced sulfur species in aqueous solution. *Environ Sci Technol* 11:1114–1120
- Podowski EL, Moore TS, Zelnio KA, Luther GW III, Fisher CR (2009) Distribution of diffuse flow megafauna in two sites on the Eastern Lau Spreading Center, Tonga. *Deep Sea Res I* 56:2041–2056
- Podowski EL, Ma S, Luther GW III, Wardrop D, Fisher CR (2010) Biotic and abiotic factors affecting the distributions of megafauna in diffuse flow on andesite and basalt along the Eastern Lau Spreading Center, Tonga. *Mar Ecol Prog Ser* 418:25–45
- Pyzik AJ, Sommer SE (1981) Sedimentary iron monosulfides: kinetics and mechanism of formation. *Geochim Cosmochim Acta* 45:687–698

- Rozan TF, Theberge SM, Luther GW III (2000) Quantifying elemental sulfur (S^0) bisulfide (HS^-) and polysulfides (S_x^{2-}) using a voltammetric method. *Anal Chim Acta* 415:175–184
- Sander SG, Koschinsky A, Massoth GJ, Stott M, Hunter KA (2007) Organic complexation of copper in deep-sea hydrothermal vent systems. *Environ Chem* 4:81–89
- Sarradin PM, Waelles M, Bernagout S, Le Gall C, Sarazin J, Riso R (2009) Speciation of dissolved copper within an active hydrothermal edifice on the Lucky Strike vent field (MAR, 37°N). *Sci Total Environ* 407:869–878
- Sarrazin J, Juniper SK, Massoth G, Legendre P (1999) Physical and chemical factors influencing species distributions on hydrothermal sulfide edifices of the Juan de Fuca Ridge, northeast Pacific. *Mar Ecol Prog Ser* 190:89–112
- Scheirer DS, Shank TM, Fornari DJ (2006) Temperature variations at diffuse and focused flow hydrothermal vent sites along the northern East Pacific Rise. *Geochem Geophys Geosyst* 7:3
- Shank TM, Fornari DJ, Von Damm KL, Lilley MD, Haymon RM, Lutz RA (1998) Temporal and spatial patterns of biological community development at nascent deep-sea hydrothermal vents (9°50'N East Pacific Rise). *DSR II* 45:465–515
- Stanbury D (1989) Reduction potentials involving inorganic free radicals in aqueous solution. In: Sykes AG (ed) *Advances in inorganic chemistry*, vol 33. Academic Press, New York, pp 69–138
- Stumm W, Morgan JJ (1996) *Aquatic chemistry*, 3rd edn. Wiley, New York
- Vairavamurthy A, Manowitz B, Luther GW III, Jeon Y (1993) Oxidation state of sulfur in thiosulfate and implications for anaerobic energy metabolism. *Geochim Cosmochim Acta* 57:1619–1623
- Vazquez FG, Zhang J, Millero FJ (1989) Effect of metals on the rate of the oxidation of H_2S in seawater. *Geophys Res Lett* 16(12):1363–1366
- Vetter RD, Fry B (1998) Sulfur contents and sulfur-isotope compositions of thiotrophic symbioses in bivalve molluscs and vestimentiferan worms. *Mar Biol* 132:453–460
- Waite TJ, Moore TS, Childress JJ, Hsu-Kim H, Mullaugh KM, Nuzzio DB, Paschal AN, Tasang J, Fisher CR, Luther GW III (2008) Variation in sulfur speciation with shellfish presence at a Lau Basin diffuse flow vent site. *J Shellfish Res* 27(1):163–168
- Wang F, Tessier A, Buffle J (1998) Voltammetric determination of elemental sulfur in pore waters. *Limnol Oceanogr* 43(6):1353–1361
- Yao W, Millero FJ (1996) Oxidation of hydrogen sulfide by hydrous Fe(III) oxides in seawater. *Mar Chem* 52:1–16